



Review

Carbon Nanoparticles and Materials on Their Basis

Alina A. Kokorina ¹ , Alexey V. Ermakov ¹, Anna M. Abramova ¹, Irina Yu. Goryacheva ¹ 
and Gleb B. Sukhorukov ^{1,2,*}

¹ Department of General and Inorganic Chemistry, Saratov State University, 410012 Saratov, Russia; Alinaa.kokorina@gmail.com (A.A.K.); oualeksej@yandex.ru (A.V.E.); vostrikova2401@bk.ru (A.M.A.); goryachevaiy@mail.ru (I.Y.G.)

² School of Engineering and Materials Science, Queen Mary University of London, Mile End Road, London E1 4NS, UK

* Correspondence: g.sukhorukov@qmul.ac.uk; Tel.: +44-793-992-8158

Received: 6 August 2020; Accepted: 23 September 2020; Published: 25 September 2020



Abstract: Carbon nanoparticles (CNPs) are novel nanostructures with luminescent properties. The development of CNPs involves the elaboration of various synthetic methods, structure characterization, and different applications. However, the problems associated with the CNP structure definition and properties homogeneity are not solved and barely described in depth. In this feature article, we demonstrate the approaches for the effective separation and purification of CNPs by size and size/charge ratio. We propose a promising way for the synthesis of the uniform-size structures by the application of calcium carbonate porous microparticles as reactors with defined size. Additionally, the application of the CNPs agglomerates for controllable release systems triggered by light and in-situ synthesis of fluorescent conductive carbonaceous films on the base of polyelectrolyte multilayers are under consideration.

Keywords: carbon nanoparticles; carbon dots; luminescent nanoparticles; luminescence; gel-electrophoresis; calcium carbonate microparticles; microchamber array

1. Introduction

Carbon nanoparticles became promising luminescent nanostructures and attracted a lot of attention for researchers since they were discovered in 2004 [1,2]. CNPs have drawn considerable interest over the last years due to their good luminescence, high chemical stability, conductivity, and broadband optical absorption [3–5]. For a long period, CNPs were believed to be crystalline or amorphous carbon-based nanoparticles with sizes of 10 nm. Until very recently, a large number of works presented CNPs as a mixture of structures with similar or overlapping emission [6–8]. CNPs are considered a mixture of fluorophores responsible for the luminescent properties, or a combination of a low-luminescent carbon matrix modifying with molecular fluorophore(s). The presence of several fluorophores is significantly complicating the fundamental understanding of photophysical processes and emission properties in a blue spectral region. Thus, the development of effective ways for the separation and purification of synthetic mixture for individual fluorophores or groups of fluorophores remained to be a challenging tool. To date, the researches propose the methods of primary separation of large or small pieces from the solution. The most popular primary methods for separating colloidal suspensions are centrifugation and filtration. The small size species can be removed by dialysis. Alternatively, the purification methods like chromatography and electrophoresis lead to the obtainment of several fractions with different properties [9].

As an approach to obtain CNPs with uniform properties, the synthesis in the restricted volume of microparticles is interesting, since it allows limiting the material for each CNP formation, as well as simplifying modification, for example, using inorganic ions. The biocompatibility and ability

for biodegradation of CNPs has opened the way to be used as a substitution for traditionally used materials [10]. Nowadays, CNPs are mostly applied in sensing and bioimaging [11–13], chemical analysis [14], optoelectronic devices [15,16], catalyst design [17–19], or agriculture [20,21]. The absorption properties of aggregates of CNPs can be a useful tool for the controllable release of bioactive substances, while the hydrothermally treated polymer films can be used as emissive and conductive materials [22].

Another promising approach to broadening the horizons of CNP is a CNP-in-matrix strategy for synthesizing new materials that can promote a wide range of applications in bioimaging [23], biosensing [24,25], optoelectronics [26], and drug delivery systems [27,28] with enhanced luminescence and other properties. In combination with traditional techniques for fabrication of polymer microcontainers with versatile structure and accurately tuned properties, CNPs offer a boost in the development of theranostics systems.

This feature paper summarizes the trends in non-typical approaches for the studying and application of CNPs. These are methods of fine separation of CNP mixtures, controlled CNP synthesis and modification in the restricted volume of CaCO_3 microparticles, application of hydrothermal treatment for gold nanoparticles functionalization, application of CNP aggregates as a substitute for GNPs for laser-induced theranostics carriers opening, and modification of conductive and optical properties of polymer-based composite films. In this review, we present some advanced features of CNPs' synthesis, separation, and application.

2. Methods for Synthesis and Separation of CNPs

The synthetic approaches for carbon nanoparticles can be classified as top-down and bottom-up methods [5]. The top-down approaches are based on the breaking down of larger carbon structures into nano- and microparticles. The basic start materials such as graphene oxide, carbon nanotubes, graphitic layers, or activated carbon can be destroyed to CNPs via laser ablation, discharge, and electrochemical oxidation [29,30]. However, the significant drawbacks of the approaches mentioned above are the material expenses, harsh reaction conditions correlated with the application of strong acids, long processing time, and low homogeneity in geometry and properties [31]. Chemical oxidation is the most promising top-down approach by introducing oxygen-containing functional groups, for instance -OH and -COOH, which enhanced the hydrophilicity and the emission to the CNPs. Meanwhile, the interest to the top-down methods is waned due to the difficult control of the reaction process, low quantum yields (QYs) of obtained CNPs, and large size of nanoparticles distribution. Due to difficulties the listed above, the top-down methods are becoming less popular in recent years. However, there are a lot of studies that have demonstrated the top-down approaches in detail [5,11].

The bottom-up approach refers to the conversion of smaller carbon structures into CNPs of the desired size. The bottom-up approaches are presented by hydrothermal and solvothermal reactions, microwave pyrolysis, and ultrasonication [32]. These methods allow use of a large number of start reagents and different solvents to obtain hydrophilic or hydrophobic CNPs. In recent years, according to the literature, the dominant number of the CNPs is produced by hydrothermal or microwave synthesis. The typical procedure includes the preparation of the start reagent solution and treating at constant temperature or power. Many recent reviews are demonstrating such examples [30,32–34]. However, most of the authors applying hydrothermal or microwave approaches note the high size diversity of the reaction products. There is a range of popular methods to separate and purify the mixture of CNPs. Centrifugation and filtration are widely used for removing of large fragments such as soot from obtained CNPs suspensions, while dialysis is used to remove low molecular-weight species. Thus, these approaches could not solve the problem for obtaining homogeneous in size and properties nanoparticles. Today, effective ways for separation of the reaction mixture of CNPs to individual fractions were applied, such as exclusion chromatography and gel electrophoresis.

Exclusion chromatography with Sephadex G-25 medium desalting column was used for separation of sodium dextran sulfate (DS) based CNPs [35]. Elute separation for 48 fractions with the volume for

each fraction of 0.7 mL allowed to identify three different emission bands associated with different luminophores. The first luminophore type (type 1) appears in the start fractions of 8–15 with emission at 400–440 nm (Figure 1). The emission intensity maximum is reached at an excitation wavelength of 340 nm; a further increase of the excitation wavelength leads to the decreasing of luminescence intensity. The second luminophore type (type 2) starts to appear in fraction 10 and elutes up to 19 fractions. The emission spectra of fractions 10–19 have two emission maxima correlating with luminophore type 1 (emission at 400–420 nm) and type 2 with longer emission at 510–520 nm. The optimal excitation for the second type is over 400 nm. The third luminophore type (type 3) is characterized by a maximum emission in the long-wavelength region at 530 nm and start to appear in fraction 35. The emission maximum was achieved in fraction 39 at excitation of 500 nm. A distinctive feature of the fluorescence profile of the third luminophore type is the absence of the dependence the emission from excitation. Therefore, the presence of molecular structures in the last fractions was proposed, corresponding with small structures confirmed by TEM measurements. Thus, the exclusion chromatography allows obtaining a large number of fractions with a tunable volume.

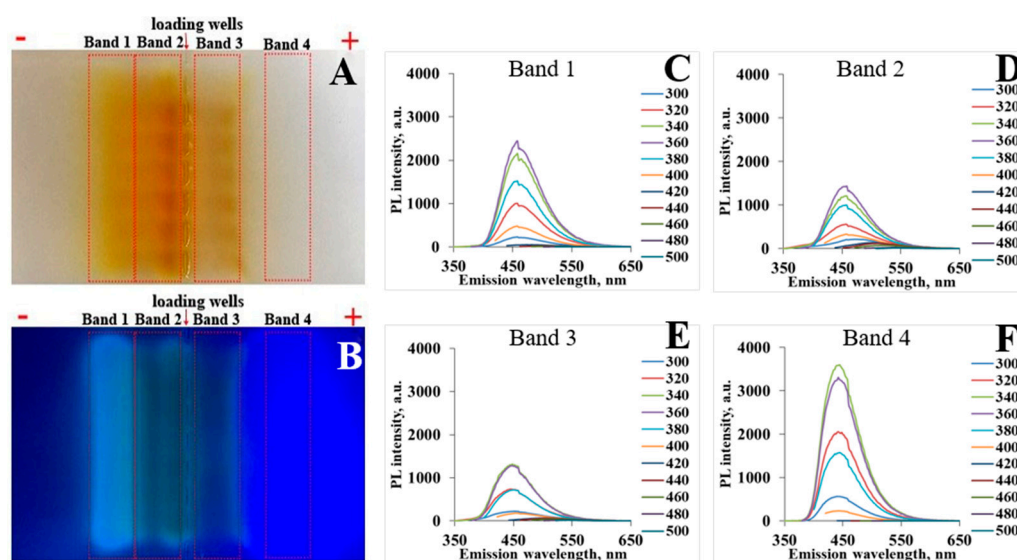


Figure 1. Gel electrophoresis separation of carbon nanoparticles (CNPs), hydrothermally obtained from citric acid (CA), and 1,2-ethylenediamine (EDA) at white light (A), and UV-light (B). Luminescent spectra of extracted bands 1 (C), 2 (D), 3 (E), and 4 (F). (Reprinted with permission from Reference [7], Copyright (2019) Elsevier).

Horizontal gel electrophoresis allows separating the mixture of CNPs by size to charge ratio. CNPs with high QY of ~67% were hydrothermally synthesized from citric acid (CA) and 1,2-ethylenediamine (EDA) with reagents molar ratio 1:1.5 (CA:EDA) [7]. The obtained dark-brown solution was separated from large soot pieces by centrifugation. For the fine separation, gel electrophoresis with 2% agarose gel was used. The authors determine four discrete bands with positive and negative charges (Figure 1A,B). The highest emission originates from a small negatively charged fluorophore. The fluorophore structure had the largest charge-to-size ratio and was identified by NMR spectroscopy as 1,2,3,5-tetrahydro-5-oxoimidazo [1,2-a]pyridine-7-carboxylic acid (IPCA). The emission maximum was at 450 nm with an absence of excitation-dependence (Figure 1F). The bands 1–3 demonstrated excitation-dependent emission typical for CNPs (Figure 1C–E). It was speculated that positive bands (1,2) contained an excess of the 1,2-ethylenediamine species and integrated fluorophore molecules. The QYs were measured for each of the bands and the largest value was around 80% for IPCA fluorophore (band 4). Band 1 had a positive charge and QY around 67%. Bands 2 and 3 had similar QYs of about 32–33% and positive and negative charges, respectively, as well as the lowest charge-to-mass ratio.

Therefore, the proposed methods allowed not only to separate the mixture to the individual components but also helped to develop the luminescence theory of CNP. CA and EDA are the most popular reagents for hydrothermal synthesis of high QY CNPs. It has been established that the luminescence of these structures originates from the organic fluorophore with a definite structure. Gel electrophoresis is a promising method for separating charge by size. However, it is important to remove the separation buffer and the agarose fragments. Size exclusion chromatography is a “purer” method due to an absence of additional buffer or other components, but leads to strong dilution of samples. Moreover, the volume of the fractions should be controlled to avoid mixing. Thus, there are two separation techniques to be used as additional tools for fine studying and understand CNP properties.

3. Synthesis of CNPs in Pores of CaCO₃ Microparticles

Encapsulation approaches have received a lot of attention because of the wide capabilities of these methods. The encapsulation process provides the concentration of reagents, or their protection creates a component microenvironment separated from the outer environment [36]. The calcium carbonate CaCO₃ porous microparticles are one of the most popular “chemical reactors”. They are formed during colloidal crystallization of inorganic salts Na₂CO₃ and CaCl₂. The resulting micro-scale reactors usually have a diameter of 1 to 6 µm and a pore size in the range of 20–60 nm [10]. These structures can be applied in engineering [37] and bioengineering [38], drug delivery [39], and chemical technology [40]. It was determined that the quality of microparticles is strongly dependent on the wide range of experimental conditions such as inorganic salts concentration, pH, temperature, and the rate of mixing the solutions. Moreover, the different molecules or their fragments can affect the CaCO₃ morphology and poses size [36]. Nowadays, the calcium carbonate microreactors became a popular technique for the controlled formation of homogeneous in size and no aggregated CNPs for improving the quality of reaction products and the avoiding separation processes.

The CNPs of uniform sizes ~3.7 nm were synthesized from DS by the hydrothermal method in pores of CaCO₃ reactors [10]. The synthesis of CNPs in pores of CaCO₃ reactors included three studies: coprecipitation of solutions of inorganic salts and DS solution, thermal treatment, and the removal of CaCO₃ matrix. The obtained CaCO₃ microparticles with DS in pores were hydrothermally treated at 200 °C for 3 h (Figure 2). After the synthesis, the color of microparticles was changed from white to brown with an absence of soot. The microparticles were dissolved to extract CNPs and three fractions were obtained. The fractions 1 and 3 had different luminescence at 420 and 460, respectively while the second fraction had both emission maxima. Raman spectra were distinctively different for the fractions. The first fraction contained a narrow D band (1350 cm⁻¹) and G bands (1580–1600 cm⁻¹) similar to graphene oxide. The broadening of D-band and the gradual reduction of intensity appears in the fractions 2 and 3 that corresponds with increasing bond-angle disorder and reduction in the number of six-fold rings in the structure of these fractions. Moreover, fractions 2 and 3 also had additional features at around 1200 and 1450 cm⁻¹ corresponding with C-C stretching modes in hydrocarbon chains and CH₂ scissoring mode, respectively. A detailed analysis of obtained data with different concentrations of DS (2, 5, and 10 mg/mL) demonstrated that a limited volume synthesis can reduce the influence of the reagents concentration and synthesis conditions on the luminescent properties of CNPs.

Moreover, the pores of CaCO₃ microparticles can be used as a “nanoscale pot” for the better conversion of raw materials into the product. Thus, the pores of CaCO₃ microparticles were also used for the synthesis of CNPs modified by Tb³⁺ ions [41]. Hydrothermal treatment of DS and TbCl₃ solutions as well as adding a TbCl₃ solution to the previously prepared CNPs, did not demonstrate any evidence of CNP modification with Tb³⁺ ions. The third method involved a simultaneous co-precipitation of DS and TbCl₃ solutions in the pores of CaCO₃ reactors with following hydrothermal treatment. The last fourth method included the stage of TbCl₃ solution freezing to the hydrothermally treated CaCO₃ reactors with incorporated CNPs. The shortest lifetime of Tb emission (0.206 ± 0.004 ms) and the largest increase of Tb emission, confirming the most effective Tb-CNPs coupling, was observed

in the system exploiting freezing-induced loading Tb together with carbon source inside the pores. The optimal excitation for energy transfer was 320–340 nm. Thus, freezing-induced loading of cations into CNPs using CaCO_3 microparticles is suggested as a promising approach for the induction of active components into CNPs. The obtained long-lived CNPs can be potentially used for time-resolved imaging or visualization in living biological samples where time-resolved luminescence microscopy is required.

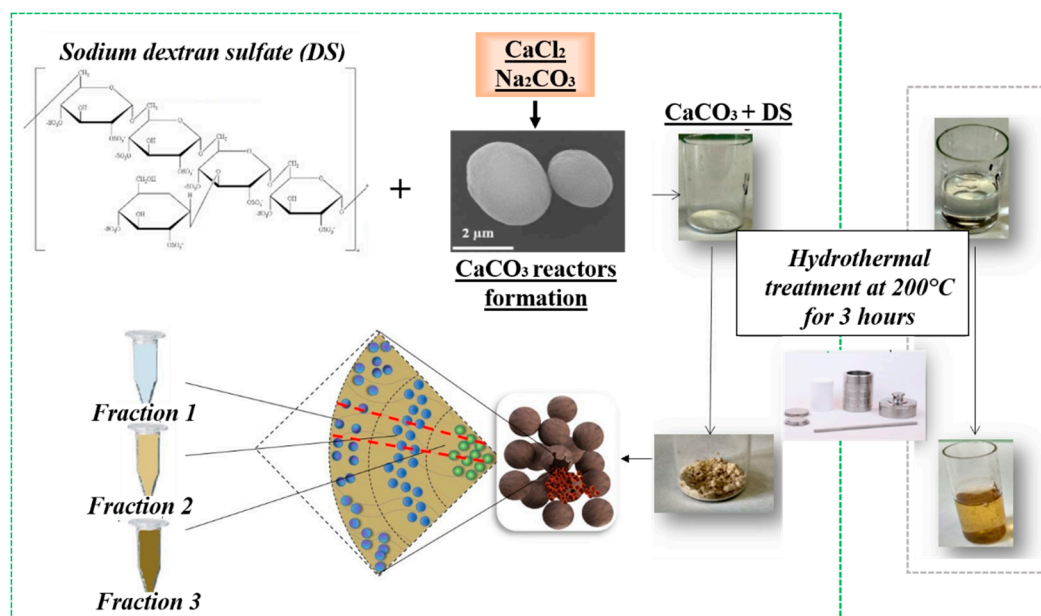


Figure 2. A schematic illustration of CNPs formation in CaCO_3 reactors (left) and bulk solution (right). (Adapted with permission from Reference [10], Copyright (2018) Nature Publishing Group).

Biocompatible, thermal stability and easy dissolution of CaCO_3 microparticles by the low concentration of ethylenediaminetetraacetic acid or hydrochloric acid are the significant advantages of this approach. Moreover, these facts made it suitable for immobilization of the biomolecules where the sensitivity of the biocompound is often a serious problem. Besides, the high surface area of $8.8 \text{ m}^2 \text{ g}^{-1}$ and pore sizes of 20–60 nm lead to immobilization of a relatively high amount of start material for the formation of CNPs.

4. Application of Hydrothermal Treatment for Gold Nanoparticles Modification

Hydrothermal synthesis of CNPs directly from biologically active compounds is widely studied [42–44]. At the same time, this approach can be used to modify the surface of other nanoparticles. Folic acid (FA) was used for hydrothermally modification of citrate reduced gold nanoparticles (GNPs) [45]. FA is one of the water-soluble B vitamins. It is an essential component for the processes of DNA and RNA synthesis, as well as in the processes of cell division. Significant interest in FA is associated with targeting cancer cells due to overexpression of folate receptors compared to normal healthy cells [46]. FA was used for modification of GNPs by hydrothermal treatment at 200°C for 1 h and treated GNPs had a bright luminescence at 450 nm (Figure 3A,B). The developed protocol avoids extra chemicals and simplifies the methodology for the eco-friendly modification of nanoparticles. An increase of the luminescent intensity (comparing with initial FA) after hydrothermal treatment was associated with the separation of “internal FA quencher” of para-aminobenzoic acid (PABA) fragment from the luminescent pterin part of FA. It is important to note that the shape and position of the luminescent maxima keep the same position as can be clearly seen from the normalized spectra (Figure 3C), confirming the stability of the pterin luminophore. After the hydrothermal treatment, the solution had the typical absorption band of FA (and pterin) ($\lambda_{\text{max}} = 282 \text{ nm}$) and

a maximum surface plasmon resonance of GNP at 525 nm. The interaction of GNPs with FA was confirmed by the change of the average hydrodynamic diameter and zeta-potential from -46 mV to -10 mV. Moreover, the biological properties of FA with GNPs after hydrothermal synthesis were analyzed by interaction with specific anti-FA antibodies. The control experiment was realized by the interaction with non-specific mouse IgG, bovine serum albumin (BSA), and an empty well. After the reaction, the characteristic absorbance band at 530 nm was determined. The obtained results confirm the presence of the FA fragments on the surface of the GNPs and the preservation of their ability to form immunocomplex with specific antibodies.

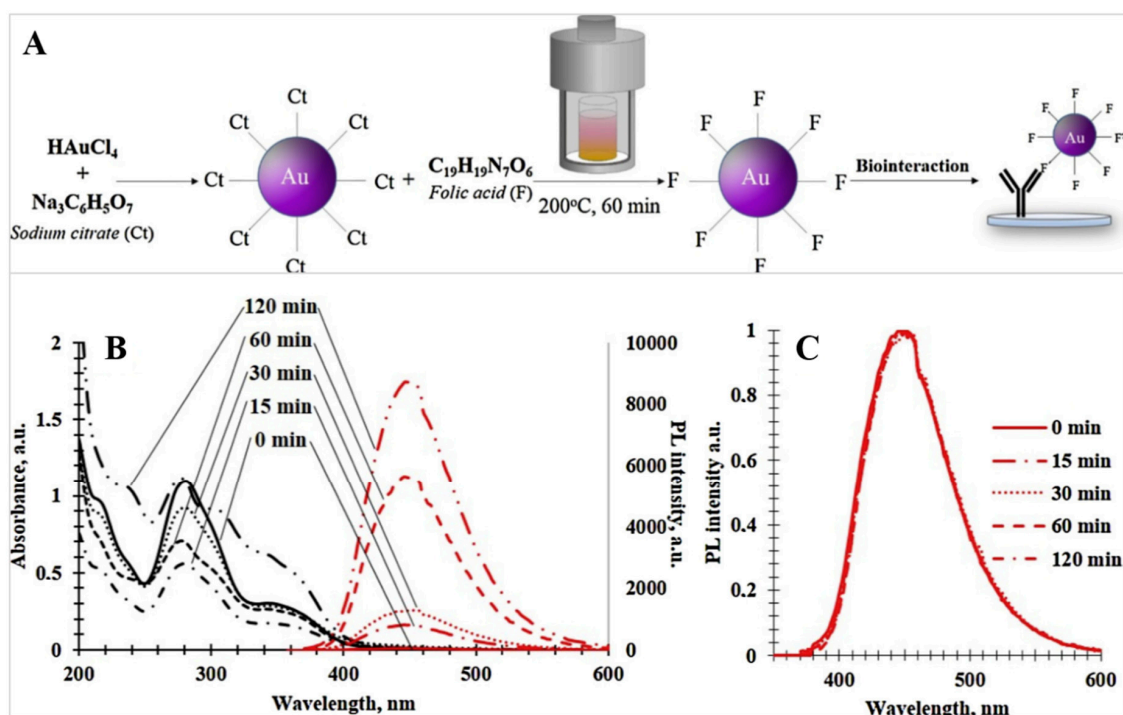


Figure 3. Scheme of GNPs synthesis, functionalization, and interaction with antibody (A); the absorbance (black) and emission (red) maxima of FA solutions after hydrothermal treatment at a different time (B); normalized emission spectra (C) (Adapted with permission from Reference [45], Copyright (2019) Elsevier).

Thus, the demonstrated hydrothermal approach can be possibly used for the further stabilization and modification of other types of nanoparticles such as silica nanoparticles, quantum dots, graphene oxide, carbon nanotubes, etc., with folate or a large variety of biologically active compounds. This is a significant way for the facile synthesis of labels for the immunoassay, bioimaging of cells or sensors for chemical analysis. The proposed approach excludes the necessity for the application of specific linkers and purification steps.

5. Application of CNPs Aggregates for Laser-Induced Cargo Release

Luminescence is one of the most useful property of CNPs that have been applied in numerous works. CNPs have proved high efficacy in a variety of tasks related to bioimaging due to strong luminescence. However, as other carbon-based materials, CNPs also has the ability to absorb light energy and convert it to heat over a wide range of wavelengths, including near infrared (NIR). Considering the high biocompatibility of CNPs in comparison to other light-absorbing materials such as graphene, carbon nanotubes and metal nanoparticles (for example, Au nanoparticles) CNPs represent a promising alternative to these materials in terms of photothermal processes.

When embedded into the shells of microcontainers, CNPs enable the release of cargo in response to light treatment. Sindeeva and co-workers successfully applied CNPs as an alternative to GNPs as a component in a promising drug depot system (Figure 4) [22]. The CNPs were synthesized using a traditional hydrothermal procedure from DS at a high concentration of 10 mg/mL at 200 °C for 3 h and re-dispersed in non-polar organic solvent resulting in a suspension of CNPs aggregates. CNPs aggregate suspension was mixed with a polylactic acid in a non-polar solvent followed by the formation of a hollow microchambers' arrays through a facile procedure of dip coating described elsewhere.

The microchamber array (MCA) is a modern controlled delivery system for a range of biologically active compounds [47]. The MCA was formed from polylactic acid (PLA) with great biocompatibility and biodegradability which in a combination with CNPs makes the system fully safe in terms of systemic- and cyto-toxicity. CNP aggregates embedded in microchamber shells demonstrate a high-temperature response to NIR-light treatment comparable to in similar systems based on plasmon-resonance of GNPs [22,48] and graphene oxide flakes [49,50]. It is very important to find a biodegradable material that traps light in the therapeutic window from 650 to 1350 nm, characterized by high transparency of biological tissues. Although gold nanostructures are the most well-known and widely applied light-responsive material, they have issues with biocompatibility and cytotoxicity, and they are not biodegradable. CNPs aggregates embedded into the structure of MCA shells were shown to facilitate site- and time-specific controlled opening under NIR-laser exposure that proves the applicability of CNPs as a promising alternative for inorganic materials like gold nanostructures. The application of CNPs aggregates as light-sensitive agents for controlled release of encapsulated materials from polymeric microcapsules has shown a stable cargo release at 785 nm and 830 nm lasers [22,51]. The principle of cargo release is based on the rapture of the polymeric shells in response to extreme heating of the light-harvesting agents which induces destruction of the polymer structure on the particle/polymer interface.

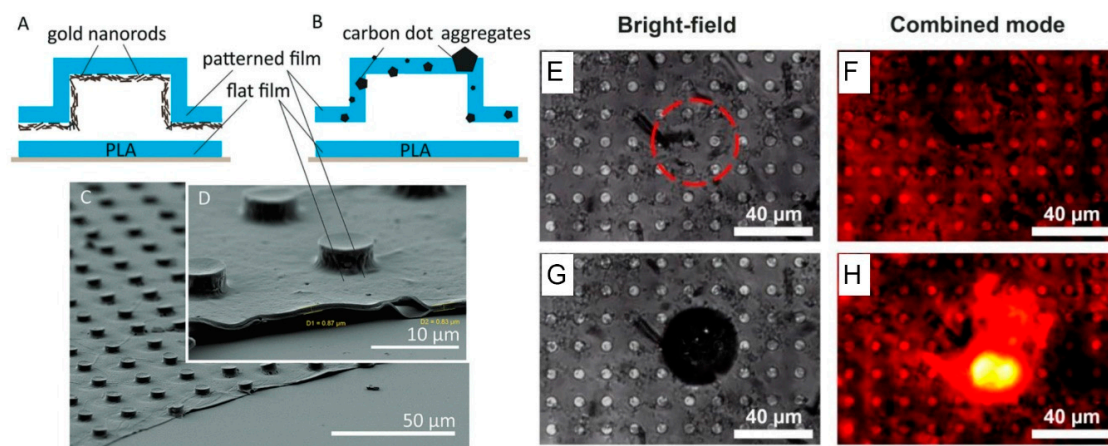


Figure 4. Left: Scheme of the gold nanorods (A) and carbon nanoparticles (B) location in the polylactic microchamber array. Typical SEM images of a polylactic microchamber array with gold nanorods (C) and carbon nanoparticles (D) (Reprinted with permission from Reference [11], Copyright (2018) The Royal Society of Chemistry); Right: Increased fluorescence of Nile Red dye after the release of hydrogen peroxide due to oxidation process in bright field (E,G) and combined mode (F,H) (Reprinted with permission from Reference [51], Copyright (2020) The Royal Society of Chemistry).

Numerous studies have shown the highly localized nature of the heating caused by photothermal treatment, which is limited to nano- and submicron-environments. The high localization of the process enables the maintaining of the cargo properties and helps to avoid obstructing biological objects contacting the surface of the microchambers' arrays. The release from the microchamber arrays with CNP aggregates under laser exposure of different compounds, such as fluorescent cargo (FITC-dextran) [22] and a solid compound containing hydrogen peroxide (sodium percarbonate

$\text{Na}_2\text{CO}_3 \cdot 1.5\text{H}_2\text{O}_2$) [51] were demonstrated (Figure 4). Hydrogen peroxide has been shown to exhibit oxidizing properties when released from individual microchambers. Multiple studies on cell adhesion and viability have demonstrated biocompatibility and viability of cells on top of hybrid CNPs-modified microchambers.

Thus, CNPs can be used as more affordable, biocompatible, and biodegradable material for targeted drug delivery systems. They demonstrated the same to GNPs efficiency for the controlled opening of MCAs under laser exposure. Moreover, the CNPs similar to GNPs can be applied for targeted release from single or several chambers. The proposed technique can be potentially used for cellular engineering for the local release of chemicals in individual cells under laser exposure.

6. Application of in Situ Formed Carbon Nanostructures for Functionalization of Polymer-Based Materials

Depending on the type of CNPs, they can exhibit high conductivity, which can be referred to the graphene-like structure of the particles. Recent advances in the fabrication of new devices based on functional polymer-based composites such as optoelectronic devices [52], organic light-emitting diodes (which demand materials with high luminescence properties) [53], and high-performance electrodes for supercapacitors [54] have proved the applicability of such composites. Usually polyelectrolytes are altered with quantum dots to give additional properties to the composite film [55,56]. Ermakov et al. reported in situ formation of carbon nanostructures via hydrothermal carbonization of the layer-by-layer assembled film on the base of 20, 40, and 80 bilayers of poly(sodium 4-styrenesulfonate) (PSS) and poly(allylamine hydrochloride) (PAH) (Figure 5) [57].

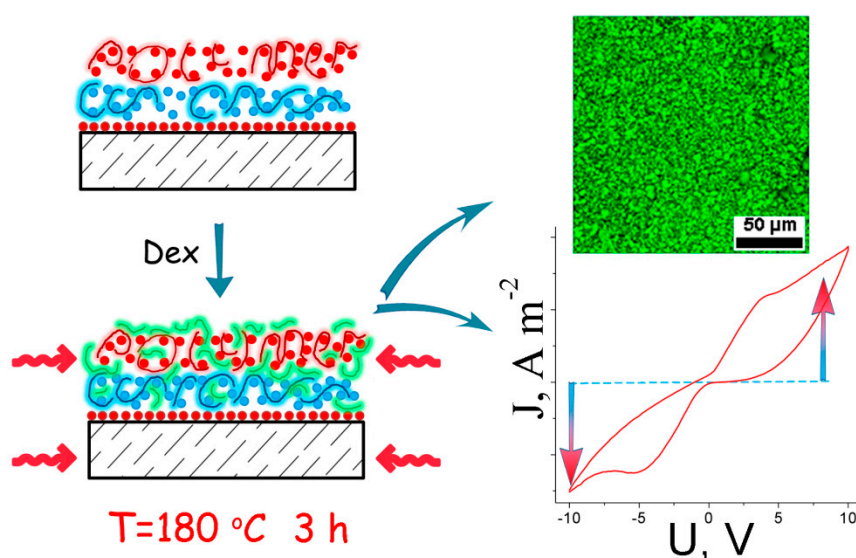


Figure 5. Scheme of layer-by-layer polymer film formation, and CLSM image and current-voltage characteristics of the 40 bilayers film (Adapted with permission from Reference [57]. Copyright (2019) John Wiley and Sons).

After the formation of the film, it was additionally infiltrated by DS solution to enrich structure with carbon. LbL-assembly technique is beneficial because the structure and properties of such films can be accurately tuned accordingly to the task. The resulted films were employed as carbon-rich matrices to nucleate and grow carbon nanostructures during the hydrothermal procedure. Fourier-transform infrared (FTIR) and Raman spectra showed the thermal treatment to provide the transition of the film structure from a molecular-like film structure to “extended carbons” with aromatic rings as a part of the structure. In combination with SEM images and analysis of the luminescent properties of the film, it was concluded that carbon nanostructures are formed on top of the film structure. After thermal treatment microcapsules exhibit Furthermore, the conductivity of the film increases by two orders of magnitude to about 0.055 S cm^{-1} which is comparable to that of graphene and carbon

nanotube-based composites that may indicate high conductivity of the resulted filler. This approach represents the completely “green” and facile procedure for in situ fabrication of conducting and highly emissive material. On the top of their “green” properties, these films are transparent and biodegradable that makes them beneficial in tasks at the junction of physics and biomedicine such as body implantable electronics.

A similar procedure was used to synthesize CNP in the shells of polyelectrolyte microcapsules. Microcapsules based on polysaccharides were used as templates for the in situ synthesis of fluorescent CNPs. After thermal treatment microcapsules exhibit strong luminescence in the blue spectral region as well as reduced permeability and ultrasound sensitivity that represent in situ synthesis of fluorescent carbon dots/polyelectrolyte nanocomposite microcapsules with reduced permeability and ultrasound sensitivity an attractive alternative over the conventional dye-based capsule tracking and drug delivery vehicles [58].

7. Conclusions

In this overview, we have summarized the progress and several trends of synthesis and application of CNPs. The bottom-up methods, and in particular, the most popular hydrothermal approach, lead to the obtain of the mixture of CNPs of different size and structure. Thus, the importance of proper purification and characterization cannot be underestimated. The effective approaches for fine separation such as size-exclusion chromatography and gel electrophoresis has been demonstrated in recent works. These methods helped to understand the little-known origin of luminescence properties. There are technologies for the controlled synthesis of CNPs such as the calcium carbonate microparticles reactors, are necessary for the synthesis of uniform-size CNPs. Together with that, the CaCO_3 reactors can be used as a “nanoscale pot” for the effective production of terbium modified CNPs. The CNPs and Tb interaction was confirmed by size-exclusion chromatography and both of Tb luminescent lifetime decreasing and the enhanced of Tb luminescent intensity. This approach was shown as successful application of FA-based CNPs for surface functionalization of GNPs. The produced modified GNPs retained properties of precursor molecules as biological ligand and show specific binding to the anti-FA antibody.

Two strategies for the fabrication of CNPs confined in the host matrices were investigated based on two host matrices (PLA and multilayer polyelectrolytes). It has been found that CNPs in a polymer backbone endow the composite material with a number of excellent properties such as luminescence, conductivity and absorption. While been embedded into the polymer shells of microcontainers the CNPs were shown to produce a photothermal effect under NIR laser treatment. CNPs-mediated release of functional cargo was shown to occur in response to low power NIR laser with properties of the cargo maintained after the release process. CNPs were demonstrated to be an effective alternative to traditional non-organic fillers applied in functional composites such as gold nanostructures, but with a high level of biocompatibility.

We believe that the perspective area of CNPs application is much wider than just luminous nanomaterials and their use will make it possible to take a step towards greener and biocompatible technologies.

8. Future Perspectives

General evidence of the superior properties of carbon nanoparticles such as fluorescence, conductivity, absorbance and others in combination with great biocompatibility open a venue for applications in various fields of science in the future. This combination of properties shows the principal possibility to detect carbon nanoparticles and structures CNDs are components of with electromagnetic irradiation in different wavelengths ranging from UV to radio-waves. In this way, drug delivery systems can be accompanied by the detection of these drug carriers within the body with intact radio waves, which is important to control drug delivery and release in theranostics fashion with combining imaging and therapy. Furthermore, carbon dots can potentially provide additional

functions such as hypothermia induced by external fields as alternatives to conductive agents such as gold nanoparticles and carbon nanotubes. These features can make carbon nanoparticles one of the most prevalent materials in biomedicine.

Funding: This research was funded by the Russian Science Foundation, grant number 16-13-10195.

Conflicts of Interest: The authors declare no conflict of interest.

References

- Xu, X.; Ray, R.; Gu, Y.; Ploehn, H.J.; Gearheart, L.; Raker, K.; Scrivens, W.A. Electrophoretic analysis and purification of fluorescent single-walled carbon nanotube fragments. *J. Am. Chem. Soc.* **2004**, *126*, 12736–12737. [[CrossRef](#)] [[PubMed](#)]
- Li, M.; Chen, T.; Gooding, J.J.; Liu, J. Review of carbon and graphene quantum dots for sensing. *ACS Sensors* **2019**, *4*, 1732–1748. [[CrossRef](#)] [[PubMed](#)]
- Reckmeier, C.J.; Schneider, J.; Susa, A.S.; Rogach, A.L. Luminescent colloidal carbon dots: Optical properties and effects of doping [Invited]. *Opt. Express* **2016**, *24*, A312–A340. [[CrossRef](#)] [[PubMed](#)]
- Goryacheva, I.Y.; Sapelkin, A.V.; Sukhorukov, G.B. Carbon nanodots: Mechanisms of photoluminescence and principles of application. *Trends Anal. Chem.* **2017**, *90*, 27–37. [[CrossRef](#)]
- Kokorina, A.A.; Prikhozhenko, E.S.; Sukhorukov, G.B.; Sapelkin, A.V.; Goryacheva, I.Y. Luminescent carbon nanoparticles: Synthesis, methods of investigation, applications. *Russ. Chem. Rev.* **2017**, *86*, 1157–1171. [[CrossRef](#)]
- Xiong, Y.; Schneider, J.; Ushakova, E.V.; Rogach, A.L. Influence of molecular fluorophores on the research field of chemically synthesized carbon dots. *Nano Today* **2018**, *23*, 124–139. [[CrossRef](#)]
- Kokorina, A.A.; Bakal, A.A.; Shpuntova, D.V.; Kostitskiy, A.Y.; Beloglazova, N.V.; De Saeger, S.; Sukhorukov, G.B.; Sapelkin, A.V.; Goryacheva, I.Y. Gel electrophoresis separation and origins of light emission in fluorophores prepared from citric acid and ethylenediamine. *Sci. Rep.* **2019**, *9*, 1–8. [[CrossRef](#)]
- Ehrat, F.; Bhattacharyya, S.; Schneider, J.; Löf, A.; Wyrwich, R.; Rogach, A.L.; Stolarczyk, J.K.; Urban, A.S.; Feldmann, J. Tracking the source of carbon dot photoluminescence: Aromatic Domains versus molecular fluorophores. *Nano Lett.* **2017**, *17*, 7710–7716. [[CrossRef](#)]
- Kokorina, A.A.; Sapelkin, A.V.; Sukhorukov, G.B.; Goryacheva, I.Y. Luminescent carbon nanoparticles separation and purification. *Adv. Colloid Interface Sci.* **2019**, *274*, 102043. [[CrossRef](#)]
- Vostrikova, A.V.; Prikhozhenko, E.S.; Mayorova, O.A.; Goryacheva, I.Y.; Tarakina, N.V.; Sukhorukov, G.B.; Sapelkin, A.V. Thermal carbonization in nanoscale reactors: Controlled formation of carbon nanodots inside porous CaCO₃ microparticles. *Sci. Rep.* **2018**, *8*, 1–7. [[CrossRef](#)]
- Liu, M.L.; Bin Chen, B.; Li, C.M.; Huang, C.Z. Carbon dots: Synthesis, formation mechanism, fluorescence origin and sensing applications. *Green Chem.* **2019**, *21*, 449–471. [[CrossRef](#)]
- Sun, X.; Lei, Y. Fluorescent carbon dots and their sensing applications. *TrAC Trends Anal. Chem.* **2017**, *89*, 163–180. [[CrossRef](#)]
- Atabaev, T.S. Doped carbon dots for sensing and bioimaging applications: A minireview. *Nanomaterials* **2018**, *8*, 342. [[CrossRef](#)] [[PubMed](#)]
- Liu, H.; Ding, J.; Zhang, K.; Ding, L. Construction of biomass carbon dots based fluorescence sensors and their applications in chemical and biological analysis. *TrAC Trends Anal. Chem.* **2019**, *118*, 315–337. [[CrossRef](#)]
- Lim, S.Y.; Shen, W.; Gao, Z. Carbon quantum dots and their applications. *Chem. Soc. Rev.* **2015**, *44*, 362–381. [[CrossRef](#)]
- Yuan, F.; Li, S.; Fan, Z.; Meng, X.; Fan, L.; Yang, S. Shining carbon dots: Synthesis and biomedical and optoelectronic applications. *Nano Today* **2016**, *11*, 565–586. [[CrossRef](#)]
- Zhu, C.; Liu, C.; Zhou, Y.; Fu, Y.; Guo, S.; Li, H.; Zhao, S.; Huang, H.; Liu, Y.; Kang, Z. Carbon dots enhance the stability of CdS for visible-light-driven overall water splitting. *Appl. Catal. B Environ.* **2017**, *216*, 114–121. [[CrossRef](#)]
- Wu, X.; Zhu, C.; Wang, L.; Guo, S.; Zhang, Y.; Li, H.; Huang, H.; Liu, Y.; Tang, J.; Kang, Z. Control strategy on two-/four-electron pathway of water splitting by multidoped carbon based catalysts. *ACS Catal.* **2017**, *7*, 1637–1645. [[CrossRef](#)]

19. Zhu, C.; Liu, C.; Fu, Y.; Gao, J.; Huang, H.; Liu, Y.; Kang, Z. Construction of CDs/CdS photocatalysts for stable and efficient hydrogen production in water and seawater. *Appl. Catal. B Environ.* **2019**, *242*, 178–185. [[CrossRef](#)]
20. Li, Y.; Xu, X.; Wu, Y.; Zhuang, J.; Zhang, X.; Zhang, H.; Lei, B.; Hu, C.; Liu, Y. A review on the effects of carbon dots in plant systems. *Mater. Chem. Front.* **2020**, *4*, 437–448. [[CrossRef](#)]
21. Li, Y.; Gao, J.; Xu, X.; Wu, Y.; Zhuang, J.; Zhang, X.; Zhang, H.; Zheng, M.; Liu, Y.; Hu, C.; et al. Carbon dots as protective agent alleviating abiotic stresses on rice (*Oryza sativa* L.) through promoting nutrition assimilation and defense system. *ACS Appl. Mater. Interfaces* **2019**, *12*, 33575–33585. [[CrossRef](#)] [[PubMed](#)]
22. Sindeeva, O.A.; Prikhozhenko, E.S.; Bratashov, D.N.; Vostrikova, A.M.; Atkin, V.S.; Ermakov, A.V.; Khlebtsov, B.N.; Sapelkin, A.V.; Goryacheva, I.Y.; Sukhorukov, G.B. Carbon dot aggregates as an alternative to gold nanoparticles for the laser-induced opening of microchamber arrays. *Soft Matter* **2018**, *14*, 9012–9019. [[CrossRef](#)] [[PubMed](#)]
23. Cao, L.; Wang, X.; Mezziani, M.J.; Lu, F.; Wang, H.; Luo, P.G.; Lin, Y.; Harruff, B.A.; Veca, L.M.; Murray, D.; et al. Carbon dots for multiphoton bioimaging. *J. Am. Chem. Soc.* **2007**, *129*, 11318–11319. [[CrossRef](#)] [[PubMed](#)]
24. Kong, B.; Zhu, A.; Ding, C.; Zhao, X.; Li, B.; Tian, Y. Carbon dot-based inorganic-organic nanosystem for two-photon imaging and biosensing of pH variation in living cells and tissues. *Adv. Mater.* **2012**, *24*, 5844–5848. [[CrossRef](#)]
25. Campuzano, S.; Yáñez-Sedeño, P.; Pingarrón, J.M. Carbon dots and graphene quantum dots in electrochemical biosensing. *Nanomaterials* **2019**, *9*, 634. [[CrossRef](#)]
26. Guan, Q.; Su, R.; Zhang, M.; Zhang, R.; Li, W.; Wang, D.; Xu, M.; Fei, L.; Xu, Q. Highly fluorescent dual-emission red carbon dots and their applications in optoelectronic devices and water detection. *New J. Chem.* **2019**, *43*, 3050–3058. [[CrossRef](#)]
27. Hettiarachchi, S.D.; Graham, R.M.; Mintz, K.J.; Zhou, Y.; Vanni, S.; Peng, Z.; Leblanc, R.M. Triple conjugated carbon dots as a nano-drug delivery model for glioblastoma brain tumors. *Nanoscale* **2019**, *11*, 6192–6205. [[CrossRef](#)]
28. Zhou, Y.; Liyanage, P.Y.; Devadoss, D.; Rios Guevara, L.R.; Cheng, L.; Graham, R.M.; Chand, H.S.; Al-Youbi, A.O.; Bashammakh, A.S.; El-Shahawi, M.S.; et al. Nontoxic amphiphilic carbon dots as promising drug nanocarriers across the blood-brain barrier and inhibitors of β -amyloid. *Nanoscale* **2019**, *11*, 22387–22397. [[CrossRef](#)]
29. Zhi, B.; Yao, X.X.; Cui, Y.; Orr, G.; Haynes, C.L. Synthesis, applications and potential photoluminescence mechanism of spectrally tunable carbon dots. *Nanoscale* **2019**, *11*, 20411–20428. [[CrossRef](#)]
30. Sharma, A.; Das, J. Small molecules derived carbon dots: Synthesis and applications in sensing, catalysis, imaging, and biomedicine. *J. Nanobiotechnol.* **2019**, *17*, 1–24. [[CrossRef](#)]
31. Wu, Z.L.; Liu, Z.X.; Yuan, Y.H. Carbon dots: Materials, synthesis, properties and approaches to long-wavelength and multicolor emission. *J. Mater. Chem. B* **2017**, *5*, 3794–3809. [[CrossRef](#)] [[PubMed](#)]
32. Choi, Y.; Choi, Y.; Kwon, O.H.; Kim, B.S. Carbon dots: Bottom-up syntheses, properties, and light-harvesting applications. *Chem. Asian J.* **2018**, *13*, 586–598. [[CrossRef](#)] [[PubMed](#)]
33. De Medeiros, T.V.; Manioudakis, J.; Noun, F.; Macairan, J.R.; Victoria, F.; Naccache, R. Microwave-assisted synthesis of carbon dots and their applications. *J. Mater. Chem. C* **2019**, *7*, 7175–7195. [[CrossRef](#)]
34. Qu, D.; Sun, Z. The formation mechanism and fluorophores of carbon dots synthesized: Via a bottom-up route. *Mater. Chem. Front.* **2020**, *4*, 400–420. [[CrossRef](#)]
35. Kokorina, A.A.; Prikhozhenko, E.S.; Tarakina, N.V.; Sapelkin, A.V.; Sukhorukov, G.B.; Goryacheva, I.Y. Dispersion of optical and structural properties in gel column separated carbon nanoparticles. *Carbon* **2018**, *127*, 541–547. [[CrossRef](#)]
36. Volodkin, D.V.; Larionova, N.I.; Sukhorukov, G.B. Protein encapsulation via porous CaCO_3 microparticles templating. *Biomacromolecules* **2004**, *5*, 1962–1972. [[CrossRef](#)]
37. Casanova, H.; Higuera, L.P. Synthesis of calcium carbonate nanoparticles by reactive precipitation using a high pressure jet homogenizer. *Chem. Eng. J.* **2011**, *175*, 569–578. [[CrossRef](#)]
38. Li, X.; Yang, X.; Liu, X.; He, W.; Huang, Q.; Li, S.; Feng, Q. Calcium carbonate nanoparticles promote osteogenesis compared to adipogenesis in human bone-marrow mesenchymal stem cells. *Prog. Nat. Sci. Mater. Int.* **2018**, *28*, 598–608. [[CrossRef](#)]
39. Wu, Y.; Gu, W.; Xu, Z.P. Enhanced combination cancer therapy using lipid-calcium carbonate/phosphate nanoparticles as a targeted delivery platform. *Nanomedicine* **2019**, *14*, 77–92. [[CrossRef](#)]

40. Wang, X.; Shi, L.; Zhang, J.; Cheng, J.; Wang, X. In situ formation of surface-functionalized ionic calcium carbonate nanoparticles with liquid-like behaviours and their electrical properties. *R. Soc. Open Sci.* **2018**, *5*, [CrossRef]
41. Vostrikova, A.M.; Kokorina, A.A.; Demina, P.A.; German, S.V.; Novoselova, M.V.; Tarakina, N.V.; Sukhorukov, G.B.; Goryacheva, I.Y. Fabrication and photoluminescent properties of Tb³⁺ doped carbon nanodots. *Sci. Rep.* **2018**, *8*, 1–8. [CrossRef]
42. Li, F.; Li, Y.; Yang, X.; Han, X.; Jiao, Y.; Wei, T.; Yang, D.; Xu, H.; Nie, G. Highly fluorescent chiral N-S-Doped carbon dots from cysteine: Affecting cellular energy metabolism. *Angew. Chemie* **2018**, *130*, 2401–2406. [CrossRef]
43. Cailotto, S.; Amadio, E.; Facchin, M.; Selva, M.; Pontoglio, E.; Rizzolio, F.; Riello, P.; Toffoli, G.; Benedetti, A.; Perosa, A. Carbon dots from sugars and ascorbic acid: Role of the precursors on morphology, properties, toxicity, and drug uptake. *ACS Med. Chem. Lett.* **2018**, *9*, 832–837. [CrossRef] [PubMed]
44. Yang, J.; Chen, W.; Liu, X.; Zhang, Y.; Bai, Y. Hydrothermal synthesis and photoluminescent mechanistic investigation of highly fluorescent nitrogen doped carbon dots from amino acids. *Mater. Res. Bull.* **2017**, *89*, 26–32. [CrossRef]
45. Vostrikova, A.M.; Kokorina, A.A.; Mitrophanova, A.N.; Sindeeva, O.A.; Sapelkin, A.V.; Sukhorukov, G.B.; Goryacheva, I.Y. One step hydrothermal functionalization of gold nanoparticles with folic acid. *Colloids Surf. B Biointerfaces* **2019**, *181*, 533–538. [CrossRef]
46. Van Dam, G.M.; Themelis, G.; Crane, L.M.A.; Harlaar, N.J.; Pleijhuis, R.G.; Kelder, W.; Sarantopoulos, A.; de Jong, J.S.; Arts, H.J.G.; van Der Zee, A.G.J.; et al. Intraoperative tumor-specific fluorescence imaging in ovarian cancer by folate receptor- α targeting: First in-human results. *Nat. Med.* **2011**, *17*, 1315–1319. [CrossRef]
47. Kiryukhin, M.V.; Man, S.M.; Tonoyan, A.; Low, H.Y.; Sukhorukov, G.B. Adhesion of polyelectrolyte multilayers: Sealing and transfer of microchamber arrays. *Langmuir* **2012**, *28*, 5678–5686. [CrossRef]
48. Ke, H.; Wang, J.; Dai, Z.; Jin, Y.; Qu, E.; Xing, Z.; Guo, C.; Yue, X.; Liu, J. Gold-nanoshelled microcapsules: A theranostic agent for ultrasound contrast imaging and photothermal therapy. *Angew. Chemie. Int. Ed.* **2011**, *50*, 3017–3021. [CrossRef]
49. Ermakov, A.; Lim, S.H.; Gorelik, S.; Kauling, A.P.; de Oliveira, R.V.B.; Castro Neto, A.H.; Glukhovskoy, E.; Gorin, D.A.; Sukhorukov, G.B.; Kiryukhin, M.V. Polyelectrolyte–Graphene oxide multilayer composites for array of microchambers which are mechanically robust and responsive to NIR light. *Macromol. Rapid Commun.* **2019**, *40*, 1–7. [CrossRef]
50. Qi, Z.; Shi, J.; Zhang, Z.; Cao, Y.; Li, J.; Cao, S. PEGylated graphene oxide-capped gold nanorods/silica nanoparticles as multifunctional drug delivery platform with enhanced near-infrared responsiveness. *Mater. Sci. Eng. C* **2019**, *104*, 109889. [CrossRef]
51. Ermakov, A.V.; Kudryavtseva, V.L.; Demina, P.; Verkhovskii, R.; Zhang, J.; Lengert, E.; Sapelkin, A.; Goryacheva, I.Y.; Sukhorukov, G. Site-specific release of reactive oxygen species from ordered arrays of microchambers based on polylactic acid and carbon nanodots. *J. Mater. Chem. B* **2020**. [CrossRef]
52. Sharma, S.; Shrivastava, S.; Kumar, S.; Bhatt, K.; Tripathi, C.C. Alternative transparent conducting electrode materials for flexible optoelectronic devices. *Opto Electron. Rev.* **2018**, *26*, 223–235. [CrossRef]
53. Liu, L.; Ye, D.; Dong, R.; Chen, D.; Li, S.; Cao, K.; Cheng, G.; Chen, S.; Huang, W. Work function-tunable graphene-polymer composite electrodes for organic light-emitting diodes. *ACS Appl. Energy Mater.* **2020**, *3*, 4068–4077. [CrossRef]
54. Gupta, A.; Sardana, S.; Dalal, J.; Lather, S.; Maan, A.S.; Tripathi, R.; Punia, R.; Singh, K.; Ohlan, A. Nanostructured Polyaniline/Graphene/Fe₂O₃ composites hydrogel as a high-performance flexible supercapacitor electrode material. *ACS Appl. Energy Mater.* **2020**, *3*, 6434–6446. [CrossRef]
55. Kumar, D.S.; Kumar, B.J.; Mahesh, H.M. Polyelectrolyte layer-by-layer spin assembly of aqueous CdTe quantum dot multilayered thin films. *J. Alloys Compd.* **2018**, *735*, 2558–2566. [CrossRef]
56. Nifontova, G.; Krivenkov, V.; Zvaigzne, M.; Samokhvalov, P.; Efimov, A.E.; Agapova, O.I.; Agapov, I.I.; Korostylev, E.; Zarubin, S.; Karaulov, A.; et al. Controlling charge transfer from quantum dots to polyelectrolyte layers extends prospective applications of magneto-optical microcapsules. *ACS Appl. Mater. Interfaces* **2020**, *12*, 35882–35894. [CrossRef]

57. Ermakov, A.V.; Prikhozhenko, E.S.; Demina, P.A.; Gorbachev, I.A.; Vostrikova, A.M.; Sapelkin, A.V.; Goryacheva, I.Y.; Sukhorukov, G.B. Composite multilayer films based on polyelectrolytes and in situ-formed carbon nanostructures with enhanced photoluminescence and conductivity properties. *J. Appl. Polym. Sci.* **2019**, *136*, 1–8. [[CrossRef](#)]
58. Gao, H.; Sapelkin, A.V.; Titirici, M.M.; Sukhorukov, G.B. In situ synthesis of fluorescent Carbon Dots/Polyelectrolyte Nanocomposite microcapsules with reduced permeability and ultrasound sensitivity. *ACS Nano* **2016**, *10*, 9608–9615. [[CrossRef](#)]



© 2020 by the authors. Licensee MDPI, Basel, Switzerland. This article is an open access article distributed under the terms and conditions of the Creative Commons Attribution (CC BY) license (<http://creativecommons.org/licenses/by/4.0/>).